

Mini Review

Recent Development of Metal Alloy Nanostructures for Electrochemical Hydrogen Generation

*Quanli Han, Lvduo Fan and Hongqiang Wan**

School of Mechanical Engineering, Xi'an Technological University, Xian, P.R. China

*E-mail: hqwmql@sina.cn

Received: 21 April 2019 / Accepted: 6 September 2019 / Published: 29 October 2019

Alkaline electrolytic water hydrogen production is an important method for large-scale industrialized hydrogen production. Research and development of new cathode electrode materials with lower hydrogen evolution overpotential and higher hydrogen evolution catalytic activity has become an important means to solve the problem of high energy consumption and low efficiency in electrochemical hydrogen generation. At present, alloys have been proven to be the best catalytic material for hydrogen evolution from electrolytic water splitting in alkaline solution. In this review, alloy-based electrochemical catalysts for electrochemical hydrogen production are summarized. We summarize the catalysts from binary, ternary and alloy deposited substrates. The performances of the catalysts are compared and illustrated. A high catalytic activity for hydrogen evolution can be obtained from the synergistic effect of alloying elements.

Keywords: Alloy; Electrochemistry; Hydrogen generation; Electrode; Clean energy

1. INTRODUCTION

With the further development of human productivity, human demand for energy is growing. However, the environmental pollution caused by the existing petrochemical energy system and people's growing energy demand has intensified. To alleviate the pollution, human beings must change the existing energy strategy and find new and cleaner energy sources to gradually replace petroleum and fossil fuels [1,2]. Therefore, many studies have explored new energy sources [2,3]. Among these works, hydrogen energy stands out as a potential clean energy source to solve the current energy crisis and environmental pollution problems because of its high efficiency and clean and renewable characteristics [4-9].

As a clean energy, hydrogen energy can be widely used in many fields. Hydrogen is the lightest element in the periodic table of elements and has the highest mass specific energy among all elements

[10-14]. The combustion value of hydrogen is much higher than that of gasoline or natural gas, i.e., 2.7 times higher. Another important application of hydrogen energy is hydrogen power generation [15-20]. One of the most important applications is fuel cells. Because fuel cells have unique characteristics, they are regarded by scientists as the most promising technological inventions for the future. Among them, proton exchange membrane fuel cells (PEMFCs) fueled by hydrogen are most suitable for electric vehicles [21-24]. This application prospect makes it possible to manufacture large-scale electric vehicles to replace vehicles that use petrochemical energy in the automotive industry. The main factor that hinders the large-scale commercialization of PEMFCs is that the price of the fuel cells has not yet met the requirements of practical application. The two main factors in fuel cell cost are the high price of the raw materials and assembly technology, such as the use of precious metal catalysts, the cost of expensive proton exchange membranes and the processing cost of graphite double-clip plates [17,18,25-28]. PEMFCs cost approximately twice as much as gasoline and diesel engines. To enter the market, PEMFCs must have a lower cost, which depends on a reduction in the fuel cell material prices and further improvement in the fuel cell performance [29-34].

In this review, we first summarize the methods for the preparation of nanostructured alloys as catalysts. In the second part, we discuss the recent developments of nanostructured alloys for electrochemical hydrogen generation and their performance.

2. PREPARATION OF NANOSTRUCTURED ALLOYS

In general, impregnation is the most commonly used method for carbon-supported platinum. The dipping process generally includes two steps: dipping and reduction. After dissolving the metal precursor, it is mixed with activated carbon and stirred evenly. Then, the metal is reduced by a liquid phase chemical reductant or vapor phase reductant. Commonly used liquid phase reductants are N_2H_4 , $\text{Na}_2\text{S}_2\text{O}_3$, NaBH_4 and HCOOH . Gas phase reduction is generally used to reduce the impregnated material without filtering and washing and will not lead to metal loss; the cost of this method is relatively low, making it most suitable for mass production. However, the catalysts prepared by this method have poor dispersion, especially when using precursors containing Cl, because Cl cannot be completely removed and subsequently causes a lower catalyst activity.

Thermal decomposition is a method of obtaining zero-valent nonnoble metal atoms, which can be reduced from salt precursors. Hydroxyl salts are often used in nonaqueous systems. The decomposed products are very clean and easy to control in the synthesis. Iron pentacarbonyl is often used as a precursor for the synthesis of FePt alloys, in which Fe solute atoms can be reduced by controlling the reaction temperature. The FePt nanostructure is a kind of alloy that is easy to control in terms of composition, size and shape. In addition, CoPt alloy has been successfully synthesized by the decomposition of cobalt.

Deposition precipitation is a very effective method for the synthesis of catalysts ranging from monometallic to bimetallic. Organometallic precursors are generally not used in this method because organic metal compounds sometimes result in immature deposition, causing the inactivation of the resulting catalyst on the support. For example, the deposition precipitation reduction method is

conducted by a traditional wet chemical method. The hydrogen atoms adsorbed on the platinum particles react with another metal precursor, thus forming a mixture of two metal surfaces. Under the action of hydrogen, the surface mixture is decomposed to form a stable bimetallic component. This method not only forms bimetallic alloy particles but can also deposit metal on the substrate. Zhang et al. [35] reported that Ag–Au alloy nanoparticles with tunable size and composition were prepared by a replacement reaction between Ag nanoparticles and HAuCl_4 at elevated temperatures. This method of preparation has several notable advantages: (1) independent tuning of the size and composition of the alloy nanoparticles; (2) production of alloy nanoparticles in high concentrations; (3) general utility in the synthesis of alloy nanoparticles that cannot be obtained by the coreduction method.

Electrodeposition is the reduction of metal ions using electrochemical methods such as potentiostatic deposition and square wave voltammetry. The advantages of electrodeposition are low cost, low temperature and easy control of film thickness. Morinorto et al. [36] prepared Pt-Ru and Pt-Sn catalysts by electrodeposition, and their catalytic oxidation activities were compared. The experimental results showed that the two alloy catalysts had better CO toxicity resistance.

Dealloying is the preparation of catalysts by corrosion. Noble metal alloys can be synthesized if we control the order of corrosion and sacrifice inexpensive metal particles. Binary and ternary platinum alloys can also be prepared by dealloying. Alloy particles are synthesized from noble and nonnoble metals, and the proportion of nonnoble metal components is generally higher. Therefore, the measurement relationship of the alloy is $\text{Pt}_x\text{M}_{1-x}$, where $x = 0.2-0.5$. Nonnoble metals and platinum are soluble and do not aggregate in most alloys. Copper meets these conditions and is the best choice for nonnoble metals. The selective dissolution of copper from Au-Cu and Pt-Cu alloys has been studied, which leads to the formation of porous platinum nanosurfaces.

Colloidal synthesis has been proven to be an effective method to obtain monodispersed nanocatalysts. Although research in the past decades has mainly focused on the synthesis of noble metals such as gold and silver, control of the synthesis of platinum-based materials and its alloys has attracted much attention recently. Due to the existence of adsorbed organic trapping agents, platinum nanoparticles can be effectively prevented from further growth and Austenite maturation. When the trapping agent is selectively adsorbed on the platinum surface, the morphology of the nanocrystals can be controlled. By controlling the crystal surface of adsorption, the crystal surface without adsorption will have different growth rates along different directions. Solute atoms may adsorb on the platinum surface with a less protective interface, resulting in anisotropic growth. An important consideration in colloidal synthesis is that the structure of these alloys must be related to the availability of the zero-valent solute of the relevant metal in the solution during the reaction. The synthesized alloy catalysts were CoPt, CuPt, FePt, NiPt, PdPt, PtRh, and PtRu. Most metal precursors used in colloidal synthesis are inorganic and organic metal salts where the metal ions can be reduced to zero-valent atoms. Strong reductants are required to ensure that all metal precursors are reduced simultaneously at an appropriate rate of reduction. Raveendran and coworkers reported an environmentally benign method for the preparation of Au, Ag, and Au–Ag nanoparticles in water using glucose as the reducing agent and starch as the protecting agent [37]. The alloy nanoparticles prepared in this way appear to be homogeneous, and their sizes were well within the quantum size domain. Kim et al. [38] synthesized Au–Ag and Au–

Cu nanoparticles of various compositions using chloroform. Zheng et al. [39] synthesized Au–Ag alloy nanoparticles by yeast cells.

3. ALLOYS FOR ELECTROCHEMICAL HYDROGEN GENERATION

Au-based bimetallic alloys have been used for electrochemical hydrogen generation due to the excellent electroactivity of the noble metal nanoparticles. Darabdhara et al. [40] prepared Au-Pd bimetallic nanoparticles using a simple solution chemistry method. Ascorbic acid and reduced graphene oxide have been used as mild reducing agents and substrates, respectively. The onset potential of the hydrogen evolution kinetics reached -0.8 mV vs. RHE, which is competitive with commercial Pt/C catalysts. Other studies have been conducted for the preparation of Au-Pd alloys and use for the electrochemical hydrogen generation [41,42]. The combination of Au and Pt can result in a superior catalyst. Weng and coworkers reported creating AuPt alloy nanodendrites through a seedless chemical reaction by the assistance of the capping agent of 5-aminouracil-6-carboxylic acid [43]. The electroactive surface area of the formed AuPt alloy reached 30 m²g⁻¹. The Tafel slope of the AuPt alloy is 34 mV dec⁻¹. A similar material has been reported by Zhang and coworkers. They synthesized an Au-Pt alloy in carbon nanofibers using electrospinning plus an in situ thermal reduction process [44]. The superior electrochemical hydrogen generation performance can be ascribed to the well-dispersed Pt–AuNPs in the carbon nanofibers, which can promote the electron transport capability. Moreover, the excellent durability of the alloy can result in the high stability of the catalyst.

Platinum-based alloy catalysts have received attention due to the wide use of commercial Pt/C catalysts. Yang and coworkers reported a catalyst by PtCo alloy encapsulated in carbon nanofibers. The reported PtCo showed excellent performance towards electrochemical hydrogen generation. The result indicates that the PtCo alloy could approach the performance of the commercial Pt/C catalyst with a low loading content. A small Tafel slope of 28 mV dec⁻¹ was recorded during the characterization. Cao and coworkers reported a Pt/Ni alloy with a well-controlled face-centered cubic phase [45]. The overpotential of the Pt/Ni alloy is only 65 mV. Ternary electrocatalysts such as Pt–Ni–Co alloy have been prepared using a one-step formation method [46]. The catalyst exhibited a Cartesian-coordinate-like hexapod morphology and excellent performance for electrochemical hydrogen generation.

Nickel and its alloys also serve as an alternative cathode for hydrogen generation. For example, Cardona and coworkers demonstrated NiCo/Zn for hydrogen generation. A NiMoZn alloy was synthesized using a deposition method and exhibited good performance for electrochemical hydrogen generation [47]. Ni–Mo alloy was prepared using an in situ topotactic reduction method and showed a superaerophobic ability [48]. Excellent electrochemical hydrogen generation was recorded due to the ultrathin structure and tailored composition. Nickel-copper alloy encapsulated into graphitic shells was prepared using room temperature CVD [49]. The alloy exhibited a current density of 10 mA cm⁻² with an overpotential of 48 mV. NiFeCo and NiFeCoP alloys have been prepared using electrodeposition methods with different parameters for forming various compositions [44]. The results indicate that the presence of Fe and Co could lower the overpotential of the Ni-based alloys and result in superior electrochemical hydrogen generation performance. The results also indicate that the charge transfer

resistance of NiFeCo is much smaller than that of pure Ni. The addition of P in the alloy further enhances the electroactivity. Ni-Mo alloys also show excellent performance for electrochemical hydrogen generation due to their high activity catalyst performance. However, Ni-Mo suffers poor stability. The study showed that polished Ni-Mo has a lower activity than pure Ni. The monitoring study indicated the Mo leaches out during the electrochemical reaction. Therefore, the high activity of Ni-Mo alloys can be ascribed to the dealloying process. The porous structure due to the leaching of Mo could result in a poor stability [50]. Ni-S-Fe can be electrodeposited onto Cu foil and used for the hydrogen evolution reaction [51]. The results indicate that the electroactivity of the Ni-S-Fe alloy is higher than that of the Ni-S alloy. A small overpotential of 222 mV was recorded with a Tafel slope of 84.5 mV dec^{-1} .

A porous structure is favorable for electrocatalysis due to its large surface area. Therefore, some scientists are dedicated to the synthesis of porous alloys for electrochemical hydrogen generation. Hu and coworkers synthesized a porous NiMo alloy by annealing NiMoO₄ nanofibers under a hydrogen atmosphere under different temperatures [52]. Figure 1 shows the scheme for the preparation of a NiMo alloy. Due to the porous structure, the NiMo alloy can remain stable even for 12.5 days.

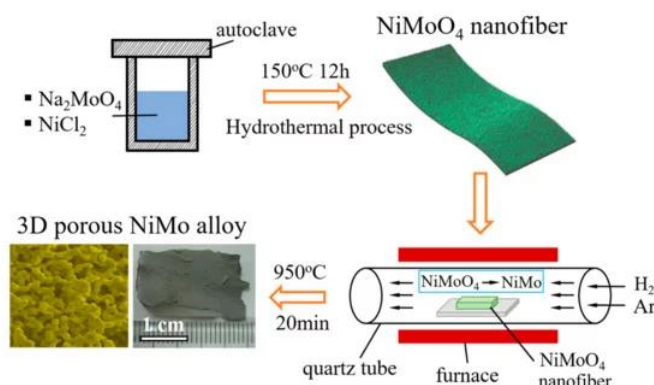


Figure 1. Schematic diagram of NiMo alloy synthesis. ([52] Copyright received from MDPI publisher)

In addition to the use of Mo as the main alloy component, the doping of Mo into Ni-Cu can also result in excellent performance for electrochemical hydrogen generation [53]. The doping of Mo can also change the morphology of the Ni-Cu alloy (Figure 2). The activity for hydrogen generation has been found to be related to the doping degree. Although 9 wt% doping of Mo showed the highest performance, the cathode showed poor stability for long-term operation. A balance can be reached when 6 wt% Mo is doped in a Ni-Cu alloy. In addition, the introduction of Ti can also enhance the alloy [54].

Ni-W alloys have outstanding electrochemical hydrogen generation performances, but their deposition process is quite slow. The assistance of magnetoelectrodeposition could significantly increase the rate [55]. The electroactivity of a Ni-W alloy could be affected by the magnetic field intensity. Characterizations showed that the W content increased when a magnetic field was applied. A unique (220) reflection was observed due to the Lorentz force-induced magnetohydrodynamic effect. Figure 3 shows the magnetoelectrodeposition of a Ni-W alloy affected by the magnetohydrodynamic effect.

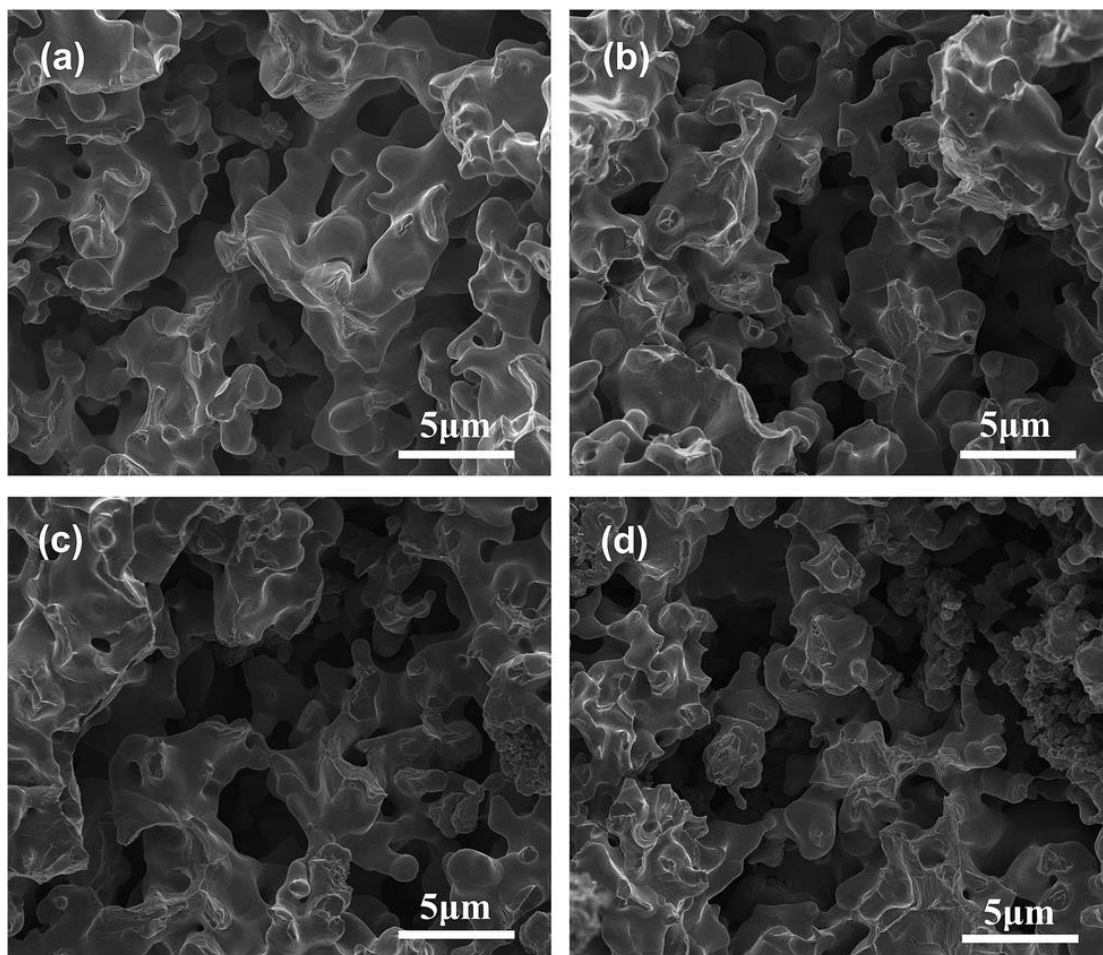


Figure 2. Morphology of the (a) Ni–Cu alloy, with (b) 3 wt%, (c) 6 wt%, (d) 9 wt% Mo doping. ([53] Copyright received from RSC publisher)

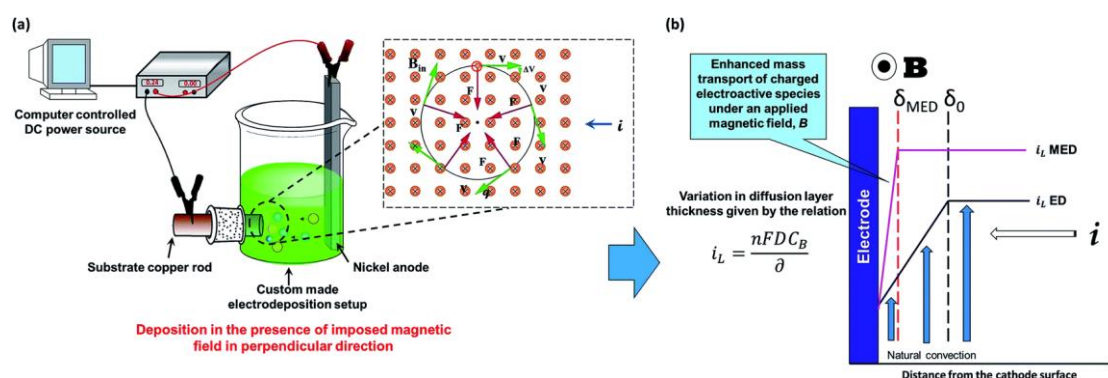


Figure 3. Scheme of magneto-electrodeposition of Ni–W alloy coating influenced by magneto-hydrodynamic effect. ([55] Copyright received from RSC publisher)

Nonprecious metal-based electrocatalysts have also been studied. Gong and coworkers reported a $\text{MoS}_{2(1-x)}\text{Se}_{2x}$ catalyst for electrochemical hydrogen generation [56]. Meiron and coworkers reported $\text{Mo}_{1-x}\text{W}_x\text{Se}_2$ with a well-controlled morphology [57]. $\text{Mo}_{1-x}\text{W}_x\text{Se}_2$ showed a superior electrochemical

hydrogen generation performance than either MoSe₂ or WSe₂. The results showed that the alloy could promote charge transfer kinetics and consequently lower the Tafel slope.

Yang and coworkers reported a one-pot synthesis method for the preparation of nonprecious metal alloy@carbon composites for electrochemical hydrogen generation [58]. MOF nanoparticles were annealed to form the FeCo alloy encapsulated in N-doped graphene. The reported electrocatalyst exhibited an 88 mV onset potential with an overpotential of 262 mV. In addition, the proposed electrocatalyst had long-term durability for 10000 cycles. RhFe alloy was prepared using a low-temperature preparation method [59]. The bimetallic alloy showed a 25 mV overpotential at a current density of 10 mA cm⁻². This result is smaller than that of the commercial Pt/C electrocatalyst. The Tafel slope is 32 mV dec⁻¹. The combination of Zn and Cr resulted in a lower overpotential than that of pure Zn [60]. Therefore, the rate of electrochemical hydrogen generation could be significantly enhanced. The performance of the Zn-Cr alloy can be altered by changing the content of Cr. A stable performance can be observed when the content ratio of Cr is between 3 and 10 mass %.

4. MECHANISMS AND OUTLOOKS

Table 1 summarizes the recent reports on alloys for electrochemical hydrogen generation. In general, the liquid phase mass transfer of hydrogen ions will not be subject to high resistance [16,19,20,57-66]. Hydrogen hydrated ions can be transported to the liquid layer on the surface of an electrode by various mass transfer actions, so this step will not be the controlling step [67,68]. Therefore, only the electrochemical reaction step, the composite desorption step or the electrochemical desorption step can be the controlling step [23,69-71]. Based on this hypothesis, scientists have proposed various hypothetical theories on the mechanism of the hydrogen evolution reaction. The slow discharge theory suggests that the electrochemical reaction step is the control step of the whole hydrogen evolution reaction process [21,72]. The slow recombination mechanism considers that the electrochemical reaction step is the control step of the whole hydrogen evolution reaction process. The electrochemical desorption theory considers that the electrochemical desorption step is the control step of the whole hydrogen evolution reaction process [73,74].

The mechanism of slow discharge suggests that the electrochemical reaction step is the control step in the whole process of hydrogen evolution [75-79]. The theoretical deduction of the mechanism of slow discharge is carried out with an affinity electrode, and the conclusions obtained are fully applicable to the oxygen evolution reaction on a mercury electrode. The mechanism is also applicable to high overpotential metals such as Pb, Cd, Zn and Ti, which cover very small hydrogen atoms [80-82]. When deducing the theoretical formula of the slow discharge mechanism on mercury electrodes, two characteristics of mercury electrodes have been used: first, the surface coverage of hydrogen atoms adsorbed on mercury electrodes is very small, so it can be considered that the surface activity of hydrogen atoms adsorbed on mercury electrodes is proportional to the surface coverage; thus, the surface coverage can be used to replace the surface activity of hydrogen atoms adsorbed on mercury electrodes [17,83-85]. Second, the mercury electrode has a uniform surface, which enables the discharge reaction of hydrogen ions on the whole electrode surface. Therefore, this mechanism is completely applicable to

mercury electrodes. However, many other metals do not have these two characteristics of mercury electrodes [86-89]. First, for most solid electrodes, their surfaces are not uniform. Second, on many metal electrodes, such as Pb, Pt, Ni and Fe, the surface coverage of adsorbed hydrogen atoms is not very small and can reach a very high value. Because there is no precondition for deducing the theoretical formula of the slow discharge mechanism on these metal electrodes, the slow discharge mechanism may not be applicable to these metals. Excessive hydrogen is adsorbed on some metal surfaces, which is closely related to the slow desorption steps of hydrogen adsorption. If the electrochemical reaction is slow and the desorption of hydrogen atoms is fast, there will be no excess hydrogen adsorbed on the surface of the electrode [86-88]. Only when the electrochemical reaction steps are fast and the desorption steps of hydrogen atoms are slow is it possible to accumulate excess hydrogen adsorbed on the surface of the electrode. Therefore, the desorption step of adsorbed hydrogen atoms is the control step of the hydrogen evolution reaction process, and the desorption step is the step involved in controlling the hydrogen evolution reaction.

Table 1. Recent developed metal alloy nanostructures for electrochemical hydrogen generation.

Materials	Onset potential	Tafel slope	Exchange current density	Reference
Au-Pd	-0.8 mV vs. RHE	29.0 mV dec ⁻¹	0.47 mA cm ⁻²	[36]
PtCo	-63 mV vs. RHE	28 mV dec ⁻¹	10.0 mA cm ⁻²	[93]
NiCo/Zn	-	80 mV dec ⁻¹	50 mA cm ⁻²	[94]
FeCo/graphene	88 mV vs. RHE	262 mV dec ⁻¹	10 mA cm ⁻²	[54]
Pt/Ni	88 mV vs. RHE	78 mV dec ⁻¹	10 mA cm ⁻²	[41]
Au-Pd	73 mV vs. RHE	165 mV dec ⁻¹	10 mA cm ⁻²	[38]
Ni-Mo	35 mV vs. RHE	-	10 mA cm ⁻²	[44]
Ni-Mo	48 mV vs. RHE	-	10 mA cm ⁻²	[45]
RhFe	25 mV vs. RHE	32 mV dec ⁻¹	10 mA cm ⁻²	[55]
Mo doped Ni-Cu	-1.33 V vs. RHE	141 mV dec ⁻¹	10 mA cm ⁻²	[49]
Mo _{1-x} W _x Se ₂	209 mV vs. RHE	51 mV dec ⁻¹	10 mA cm ⁻²	[53]
Ni-W	-0.99 vs. RHE	-	-0.97 mA cm ⁻²	[51]
Ni-S-Fe	222 mV vs. RHE	84.5 mV dec ⁻¹	10 mA cm ⁻²	[47]
Pt-AuNPs/CNFs	-235 mV vs. RHE	84.0 mV dec ⁻¹	10 mA cm ⁻²	[40]

ACKNOWLEDGEMENT

This study is funded by Shaanxi key laboratory research project (17JS060).

References

1. Y.C. Hu, Y.Z. Wang, R. Su, C.R. Cao, F. Li, C.W. Sun, Y. Yang, P.F. Guan, D.W. Ding, Z.L. Wang, *Adv. Mater.*, 28 (2016) 10293.
2. M.A. Amin, E.M. Ahmed, N.Y. Mostafa, M.M. Alotibi, G. Darabdhara, M.R. Das, J. Wysocka, J. Ryl, S.A.E. Rehim, *Acs Applied Materials & Interfaces*, 8 (2016) 23655.
3. C. Tsai, L. Hong, S. Park, J. Park, H.S. Han, J.K. Nørskov, X. Zheng, F. Abildpedersen, *Nature Communications*, 8 (2017) 15113.

4. L. Fu, A. Wang, F. Lyv, G. Lai, H. Zhang, J. Yu, C.-T. Lin, A. Yu, W. Su, *Bioelectrochemistry*, 121 (2018) 7.
5. L. Jourdin, Y. Lu, V. Flexer, J. Keller, S. Freguia, *Chemelectrochem*, 3 (2016) 581.
6. L. Fu, Y. Xu, J. Du, D. Cao, Q. Liu, *Int. J. Electrochem. Sci.*, 14 (2019) 4383.
7. G. Kumar, P. Bakonyi, G. Zhen, P. Sivagurunathan, L. Koók, S.H. Kim, G. Tóth, N. Nemestóthy, K. Bélaifibakó, *Renewable & Sustainable Energy Reviews*, 70 (2017) 589.
8. A. Thibert, F.A. Frame, E. Busby, M.A. Holmes, F.E. Osterloh, D.S. Larsen, *Journal of Physical Chemistry Letters*, 2 (2016) 2688.
9. A.M. Qureshy, M. Ahmed, I. Dincer, *Int. J. Hydrogen Energy*, 41 (2016) 8020.
10. V. Bhatt, B. Tripathi, P. Yadav, M. Kumar, *Journal of Energy Chemistry*, 12 (2017) 82.
11. V. Čolić, S. Yang, Z. Révay, I.E.L. Stephens, I. Chorkendorff, *Electrochim. Acta*, 272 (2018) 192.
12. L. Fu, A. Wang, G. Lai, W. Su, F. Malherbe, J. Yu, C.-T. Lin, A. Yu, *Talanta*, 180 (2018) 248.
13. D. Liu, T. Liu, L. Zhang, F. Qu, D. Gu, A.M. Asiri, X. Sun, *Journal of Materials Chemistry A*, 5 (2017) 3208.
14. R. Ding, Y. Liu, M. Wang, Q. Li, X. Cui, C. Wang, L. Wang, B. Lv, *Electrochim. Acta*, 248 (2017) 20.
15. P. Peljo, H. Vrabel, V. Amstutz, J. Pandard, J. Morgado, A. Santasaloarnio, D. Lloyd, F. Gumy, C.R. Dennison, K. Toghill, *Green Chemistry*, 18 (2016) 1785.
16. L. Yang, K. Wang, G. Du, W. Zhu, L. Cui, C. Zhang, X. Sun, A.M. Asiri, *Nanotechnology*, 27 (2016) 475702.
17. L. Fu, Y. Zheng, P. Zhang, H. Zhang, M. Wu, H. Zhang, A. Wang, W. Su, F. Chen, J. Yu, W. Cai, C.-T. Lin, *Bioelectrochemistry*, 129 (2019) 199.
18. Q. Li, M. Zheng, B. Zhang, C. Zhu, F. Wang, J. Song, M. Zhong, L. Ma, W. Shen, *Nanotechnology*, 27 (2016) 075704.
19. M. Sun, Y. Chen, G. Tian, A. Wu, H. Yan, H. Fu, *Electrochim. Acta*, 190 (2016) 186.
20. S.A. Rommel, D. Sorsche, S. Schönweiz, J. Kübel, N. Rockstroh, B. Dietzek, C. Streb, S. Rau, *J. Organomet. Chem.*, 821 (2016) 163.
21. L.G. Sevastyanova, V.K. Genchel, S.N. Klyamkin, P.A. Larionova, B.M. Bulychev, *Int. J. Hydrogen Energy*, 42 (2017) 16961.
22. L. Fu, A. Wang, F. Lyu, G. Lai, J. Yu, C.-T. Lin, Z. Liu, A. Yu, W. Su, *Sens. Actuators B Chem.*, 262 (2018) 326.
23. L. Fu, K. Xie, A. Wang, F. Lyu, J. Ge, L. Zhang, H. Zhang, W. Su, Y.-L. Hou, C. Zhou, C. Wang, S. Ruan, *Anal. Chim. Acta*, 1081 (2019) 51.
24. S.P. Adhikari, Z.D. Hood, K.L. More, V.W. Chen, A. Lachgar, *Chemosuschem*, 9 (2016) 1869.
25. Y. Liu, Y. Zhu, X. Fan, S. Wang, L. Yang, F. Zhang, G. Zhang, W. Peng, *Carbon*, 121 (2017) 163.
26. L. Fu, Z. Liu, J. Ge, M. Guo, H. Zhang, F. Chen, W. Su, A. Yu, *J. Electroanal. Chem.*, 841 (2019) 142.
27. R. Krishna, D.M. Fernandes, C. Dias, J. Ventura, C. Freire, E. Titus, *Int. J. Hydrogen Energy*, 41 (2016) 11498.
28. L. Fu, A. Wang, G. Lai, C.-T. Lin, J. Yu, A. Yu, Z. Liu, K. Xie, W. Su, *Microchim. Acta*, 185 (2018) 87.
29. W. Miran, M. Nawaz, J. Jang, D.S. Lee, *Water Res.*, 117 (2017) 198.
30. L. Fu, A. Wang, W. Su, Y. Zheng, Z. Liu, *Ionics*, 24 (2018) 2821.
31. R. Dom, L.R. Baby, H.G. Kim, P.H. Borse, *Int. J. Hydrogen Energy*, 42 (2017) 5758.
32. M.S. Koo, K. Cho, J. Yoon, W. Choi, *Environ. Sci. Technol.*, 51 (2017) 6590.
33. E. Pastor, F.L. Formai, M.T. Mayer, S.D. Tilley, L. Francàs, C.A. Mesa, M. Grätzel, J.R. Durrant, *Nature Communications*, 8 (2017) 14280.
34. X. Shi, S. Siahrostami, G.L. Li, Y. Zhang, P. Chakthranont, F. Studt, T.F. Jaramillo, X. Zheng, J.K. Nørskov, *Nature Communications*, 8 (2017) 701.
35. Q. Zhang, J.Y. Lee, J. Yang, C. Boothroyd, J. Zhang, *Nanotechnology*, 18 (2007) 245605.

36. Y. Morimoto, E.B. Yeager, *J. Electroanal. Chem.*, 441 (1998) 77.
37. P. Raveendran, J. Fu, S.L. Wallen, *Green Chemistry*, 8 (2006) 34.
38. M.-J. Kim, H.-J. Na, K.C. Lee, E.A. Yoo, M. Lee, *J. Mater. Chem.*, 13 (2003) 1789.
39. D. Zheng, C. Hu, T. Gan, X. Dang, S. Hu, *Sensors and Actuators B: Chemical*, 148 (2010) 247.
40. G. Darabdhara, M.A. Amin, G.A. Mersal, E.M. Ahmed, M.R. Das, M.B. Zakaria, V. Malgras, S.M. Alshehri, Y. Yamauchi, S. Szunerits, *Journal of Materials Chemistry A*, 3 (2015) 20254.
41. L. Fu, Y. Zheng, P. Zhang, J. Zhu, H. Zhang, L. Zhang, W. Su, *Electrochem. Commun.*, 92 (2018) 39.
42. A. Abbaspour, F. Norouz-Sarvestani, *Int. J. Hydrogen Energy*, 38 (2013) 1883.
43. X. Weng, Y. Liu, K.-K. Wang, J.-J. Feng, J. Yuan, A.-J. Wang, Q.-Q. Xu, *Int. J. Hydrogen Energy*, 41 (2016) 18193.
44. V. Bachvarov, E. Lefterova, R. Rashkov, *Int. J. Hydrogen Energy*, 41 (2016) 12762.
45. L. Fu, M. Wu, Y. Zheng, P. Zhang, C. Ye, H. Zhang, K. Wang, W. Su, F. Chen, J. Yu, *Sens. Actuators B Chem.*, 298 (2019) 126836.
46. L. Fu, Y. Huang, W. Cai, H. Zhang, J. Yang, D. Wu, W. Su, *Ceram. Int.*, 44 (2018) 19926.
47. X. Wang, R. Su, H. Aslan, J. Kibsgaard, S. Wendt, L. Meng, M. Dong, Y. Huang, F. Besenbacher, *Nano Energy*, 12 (2015) 9.
48. Q. Zhang, P. Li, D. Zhou, Z. Chang, Y. Kuang, X. Sun, *Small*, 13 (2017) 1701648.
49. Y. Shen, Y. Zhou, D. Wang, X. Wu, J. Li, J. Xi, *Advanced Energy Materials*, 8 (2018) 1701759.
50. M. Schalenbach, F.D. Speck, M. Ledendecker, O. Kasian, D. Goehl, A.M. Mingers, B. Breitbach, H. Springer, S. Cherevko, K.J.J. Mayrhofer, *Electrochim. Acta*, 259 (2018) 1154.
51. Y. Wu, H. He, *Int. J. Hydrogen Energy*, 43 (2018) 1989.
52. K. Hu, S. Jeong, M. Wakisaka, J.-i. Fujita, Y. Ito, *Metals*, 8 (2018) 83.
53. L. Yu, T. Lei, B. Nan, J. Kang, Y. Jiang, Y. He, C. Liu, *RSC Advances*, 5 (2015) 82078.
54. J. Panek, J. Kubisztal, B. Bierska-Piech, *Surf. Interface Anal.*, 46 (2014) 716.
55. L. Elias, P. Cao, A.C. Hegde, *RSC Advances*, 6 (2016) 111358.
56. Q. Gong, L. Cheng, C. Liu, M. Zhang, Q. Feng, H. Ye, M. Zeng, L. Xie, Z. Liu, Y. Li, *ACS Catalysis*, 5 (2015) 2213.
57. O.E. Meiron, V. Kuraganti, I. Hod, R. Bar-Ziv, M. Bar-Sadan, *Nanoscale*, 9 (2017) 13998.
58. Y. Yang, Z. Lun, G. Xia, F. Zheng, M. He, Q. Chen, *Energy & Environmental Science*, 8 (2015) 3563.
59. L. Zhang, J. Lu, S. Yin, L. Luo, S. Jing, A. Brouzgou, J. Chen, P.K. Shen, P. Tsiakaras, *Applied Catalysis B: Environmental*, 230 (2018) 58.
60. T. Boiadjeva-Scherzer, H. Kronberger, G. Fafilek, M. Monev, *J. Electroanal. Chem.*, 783 (2016) 68.
61. G. Ye, Y. Gong, J. Lin, B. Li, Y. He, S.T. Pantelides, W. Zhou, R. Vajtai, P.M. Ajayan, *Nano Lett.*, 16 (2016) 1097.
62. D. Xue, Q.Y. Lv, C.N. Lin, S.Z. Zhan, *Polyhedron*, 117 (2016) 300.
63. A.K. Mengele, S. Kaufhold, C. Streb, S. Rau, *Dalton Transactions*, 45 (2016) 6612.
64. S. Min, L. Wei, Z. Qiu, W. Gang, J. Shen, *J. Power Sources*, 301 (2016) 29.
65. F. Ganci, S. Lombardo, C. Sunseri, R. Inguanta, *Renewable Energy*, 123 (2018) 117.
66. Y.A. Bustos, J.G. Rangelperaza, M.N. Rojasvalencia, E.R. Bandala, A. Álvarezgallegos, L. Vargasestrada, *Environ. Technol.*, 37 (2016) 815.
67. Z. Liu, X. Cao, B. Wang, X. Min, S. Lin, Z. Guo, X. Zhang, S. Gao, *J. Power Sources*, 342 (2017) 452.
68. T. Catal, T. Gover, B. Yaman, J. Drogueti, K. Yilancioglu, *World J. Microbiol. Biotechnol.*, 33 (2017) 115.
69. K.L. Chang, Q. Sun, Y.P. Peng, S.W. Lai, M. Sung, C.Y. Huang, H.W. Kuo, J. Sun, Y.C. Lin, *Chemosphere*, 150 (2016) 605.
70. A. Gölle, P. Görbe, A. Magyar, *Journal of Cleaner Production*, 111 (2016) 17.

71. F. Chen, L. Zhang, X. Wang, R. Zhang, *Appl. Surf. Sci.*, 422 (2017) 962.
72. C. Xu, M. Mei, W. Qi, C. Yang, G. Fan, W. Yi, D. Gao, B. Jian, Z. Yun, *Journal of Materials Chemistry A*, 6 (2018) 14380.
73. Y. Yang, H. Fei, G. Ruan, J.M. Tour, *Adv. Mater.*, 27 (2015) 3175.
74. C. Tang, R. Zhang, W. Lu, L. He, X. Jiang, A.M. Asiri, X. Sun, *Adv. Mater.*, 29 (2017) 1602441.
75. S. Choi, T.C. Davenport, S.M. Haile, *Energy & Environmental Science*, 12 (2019) 206.
76. F. Wang, Y. Li, T.A. Shifa, K. Liu, F. Wang, Z. Wang, P. Xu, Q. Wang, J. He, *Angew. Chem. Int. Ed.*, 55 (2016) 6919.
77. N.R. Manwar, R.G. Borkar, R. Khobragade, S.S. Rayalu, S.L. Jain, A.K. Bansiwala, N.K. Labhsetwar, *Int. J. Hydrogen Energy*, 42 (2017) 10931.
78. J. Yan, L. Li, Y. Ji, P. Li, L. Kong, X. Cai, Y. Li, T. Ma, S.F. Liu, *Journal of Materials Chemistry A*, 6 (2018) 12532.
79. L. Chen, H. Jiang, H. Jiang, H. Zhang, S. Guo, Y. Hu, C. Li, *Advanced Energy Materials*, 7 (2017) 1602782.
80. J.-S. Qin, D.-Y. Du, W. Guan, X.-J. Bo, Y.-F. Li, L.-P. Guo, Z.-M. Su, Y.-Y. Wang, Y.-Q. Lan, H.-C. Zhou, *J. Am. Chem. Soc.*, 137 (2015) 7169.
81. M.R. Maghami, M. esmaeil Rezadad, N.A. Ebrahim, C. Gomes, *Scientometrics*, 105 (2015) 759.
82. X. Lei, K. Yu, H. Li, Z. Tang, Z. Zhu, *The Journal of Physical Chemistry C*, 120 (2016) 15096.
83. Y. Shi, B. Zhang, *Chem. Soc. Rev.*, 45 (2016) 1529.
84. L. Youssef, S. Roualdès, J. Bassil, M. Zakhour, V. Rouessac, C. Lamy, M. Nakhl, *J. Appl. Electrochem.*, 49 (2019) 135.
85. Y. Gong, Y. Zhao, Y. Chen, Y. Wang, C. Sun, *RSC Advances*, 6 (2016) 43185.
86. Y. Yang, F. Scenini, M. Curioni, *Electrochim. Acta*, 198 (2016) 174.
87. L. Zhang, D. Liu, S. Hao, L. Xie, F. Qu, G. Du, A.M. Asiri, X. Sun, *ChemistrySelect*, 2 (2017) 3401
88. L. An, Y. Zhang, R. Wang, H. Liu, D. Gao, Y.-Q. Zhao, F. Cheng, P. Xi, *Nanoscale*, 10 (2018) 16539.
89. Y. Liang, Q. Liu, Y. Luo, X. Sun, Y. He, A.M. Asiri, *Electrochim. Acta*, 190 (2016) 360.
90. A. Nakamura, Y. Ota, K. Koike, Y. Hidaka, K. Nishioka, M. Sugiyama, K. Fujii, *Applied Physics Express*, 8 (2015) 107101.
91. M. Masjedi-Arani, M. Salavati-Niasari, *Int. J. Hydrogen Energy*, 42 (2017) 17184.
92. B. Yang, J. Deng, G. Yu, S. Deng, J. Li, C. Zhu, Q. Zhuo, H. Duan, T. Guo, *Electrochem. Commun.*, 86 (2018) 26.
93. T. Yang, H. Zhu, M. Wan, L. Dong, M. Zhang, M. Du, *Chem. Commun.*, 52 (2016) 990.
94. I. Herraiz-Cardona, E. Ortega, L. Vázquez-Gómez, V. Pérez-Herranz, *Int. J. Hydrogen Energy*, 36 (2011) 11578